J. Appl. Comput. Mech., 4(1) (2018) 27-39
DOI: 10.22055/JACM.2017.22068.1123

ISSN: 2383-4536
jacm.scu.ac.ir

Shahid Chamran University of Ahvaz

Journal of Applied and Computational Mechanics

Research Article

Quasi-Static Transient Thermal Stresses in an Elliptical Plate due to Sectional Heat Supply on the Curved Surfaces over the Upper Face

Ishaque Khan[1], Lalsingh Khalsa[1], Vinod Varghese[2]

[1] Department of Mathematics
MG College, Armori, Gadchiroli, India, lalsinghkhalsa@yahoo.com,
[2] Department of Mathematics
Smt. Sushilabai Rajkamalji Bharti Science College, Arni, Yavatmal, India, vino7997@gmail.com

Received May 12 2017; Revised July 13 2017; Accepted for publication July 17 2017.
Corresponding author: Vinod Varghese, vino7997@gmail.com

Abstract. This paper is an attempt to determine quasi-static thermal stresses in a thin elliptical plate which is subjected to transient temperature on the top face with zero temperature on the lower face and the homogeneous boundary condition of the third kind on the fixed elliptical curved surface. The solution to conductivity equation is elucidated by employing a classical method. The solution of stress components is achieved by using Goodier's and Airy's potential function involving the Mathieu and modified functions and their derivatives. The obtained numerical results are accurate enough for practical purposes, better understanding of the underlying elliptic object, and better estimates of the thermal effect on the thermoelastic problem. The conclusions emphasize the importance of better understanding of the underlying elliptic structure, improved understanding of its relationship to circular object profile, and better estimates of the thermal effect on the thermoelastic problem.

Keywords: Elliptical plate, Temperature distribution, Thermal stresses, Mathieu function.

1. Introduction

The theoretical study of the heat flow within hollow elliptical structures has been of considerable practical importance in a wide range of sectors such as mechanical, aerospace, and food engineering fields for the past few decades. Unfortunately, there are only a few studies concerned with steady and transient state heat conduction problems in the elliptical objects. A short history of the research work associated with the thermoelasticity provides an insight into various approximate methods like the Ritz energy method, Galerkin's Method, finite element models, and the perturbation theory to solve the system. In the most recent literature, some researchers have undertaken studies on heat conduction analysis, which can be summarized as given below. Gupta [1] introduced a finite transform involving the Mathieu functions used for obtaining the solutions for boundary value problems involving elliptic cylinders. Sato [2] subsequently obtained the mathematical solution for the heat conduction problem of an infinite elliptical cylinder during heating and cooling considering the effect of the surface resistance. Recently, El Dhaba [3] used a boundary integral method to solve the problem of the plane uncoupled linear thermoelasticity with heat sources for an infinite cylinder with elliptical cross section which was subjected to a uniform pressure and a thermal radiation condition on its boundary. However, a few studies have been done to eliminate the thermoelastic problems successfully. Most recently, Helsing [4] formulated an elastic problem with mixed boundary conditions, that is, Dirichlet conditions on parts of

Published Online: October 27 2017

the boundary and Neumann conditions on the remaining contiguous parts, and solved it on an interior planar domain using an integral equation method. Dang and Mai [5] estimated mixed boundary value problem for a biharmonic equation of the Airy stress function which modeled a crack problem of a solid elastic plate using an iterative method. Al Duhaim et al. [6] determined the thermal stress of a mixed boundary value problem in half space by using Jones's modification of the so-called Wiener-Hopf technique. Parnell et al. [7] employed the Wiener-Hopf and Cagniard-de Hoop techniques to solve a range of transient thermal mixed boundary value problems on the half-space. Nuruddeen and Zaman [8] obtained the analytical solution of transient heat conduction in a solid homogeneous infinite circular cylinder using the Wiener-Hopf technique owing to the mixed nature of the boundary conditions. Very recently, Bhad [9,10] has obtained a few thermoelastic solutions for elliptical objects using the integral transform technique. The above reviews clearly suggest that, in contrast with the classical circular or rectangular structures case, nearly all investigators so far have focused on the thermoelastic problems in elliptical membranes either in the steady or unsteady state. In particular, there seems to be no rigorous analytical or numerical reports on the quasi-static transient response of a thin elliptical plate subjected to a thermal load. The primary purpose of the current work is to fill this gap. Both analytical and numerical techniques can be the best methodology to solve such problems. Nevertheless, it is observed that mostly numerical solutions are preferred due to either non-availability or mathematical complexity of the corresponding exact solutions. Rather, limited utilisation of analytical solutions should not diminish their merit over numerical ones; since exact solutions, if available, provide an insight into the governing physics of the problem that is often missing in any numerical solution. However, to the best of authors' knowledge, very few works have been published to determine the temperature distribution and its associated stresses in an elliptical plate with boundary conditions of radiation type on the outside surfaces with independent radiation constants. Owing to the lack of research in elliptical objects in the elliptic-cylinder coordinate system, the authors have been motivated to conduct this study using the classical method.

The object of this paper is to study the quasi-static thermal stresses in a thin elliptical plate subjected to a sectional heat supply on the upper face with the lower face kept at zero temperature. To establish the quasi-static problem formulation, the following assumptions need to be made: (i) The material of the cylinder is elastic, homogeneous, and isotropic, (ii) A thin-walled cylinder has been considered during the investigation with a ratio of the length to the thickness greater than 8, (iii) The deflection (the normal component of the displacement vector) of the mid-plane is small as compared with the thickness of the plate, and (iv) The stress perpendicular to the middle plane is small compared with the other stress components and may be neglected in the stress-strain relations. The success of this research mainly lies in the analytical procedures which present a much simpler approach for optimisation of the design regarding the material usage and performance in the engineering problem, particularly in the determination of the thermoelastic behaviour in the elliptical disc engaged as the foundation of pressure vessels, furnaces, etc. Actually, by considering a circle as a special kind of ellipse, it is shown that the temperature distribution and history in a circular solution can be derived as a special case of the present mathematical solution for the elliptical disc.

2. Formulation of the problem

It is assumed that a thin elliptical plate is occupying the space $D:\{(\xi,\eta,z)\in R^3:\ \ 0<\xi<\xi_0,\ 0<\eta<2\pi,\ -\ell/2<z<\ell/2\}$ under unsteady-state temperature field with no internal heat source within it. The geometry of the plate as shown in Fig. 1 indicates that an elliptic coordinate system (ξ,η,z) is the most appropriate choice of the reference frame, which is related to the rectangular coordinate system (x,y,z) by the relation $x=c\cosh\xi\cos\eta,\quad y=c\sinh\xi\sin\eta,\ z=z$.

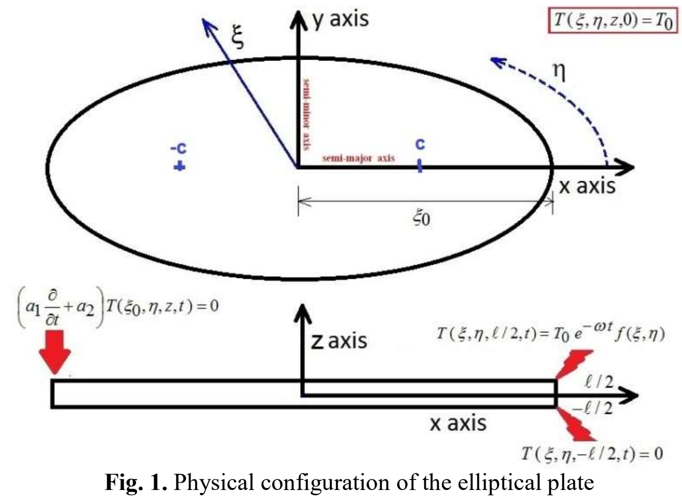

Fig. 1. Physical configuration of the elliptical plate

The length $2c$ is the distance between its common foci as shown in the geometrical configuration described in Fig. 1 which can be defined as $2c=2\sqrt{a^2-b^2}$. The curves $\eta=$ constant represent a family of confocal hyperbolas, while the curves

$\xi =$constant constitute a family of confocal ellipses. Both sets of curves intersect each other orthogonally at every point in space. The geometry parameters are given as $\xi \in [0,\xi_0]$, $\eta \in [0,2\pi)$, and $z \in [-\ell/2, \ell/2]$. The plate is subjected to the arbitrary initial temperature over the upper surface $(z = \ell/2)$ with the lower surface $(z = -\ell/2)$ at zero temperature and boundary condition of the third kind on the curved surface; Under these prescribed conditions, the quasi-static thermal stresses are required to be determined.

2.1 Heat conduction of the problem

The governing differential equation for heat conduction and boundary conditions can be defined as:

$$\frac{1}{\kappa}\frac{\partial}{\partial t}(\xi,\eta,z,t) = h^2\left(\frac{\partial^2}{\partial \xi^2}+\frac{\partial^2}{\partial \eta^2}\right)T(\xi,\eta,z,t)+\frac{\partial^2}{\partial z^2}T(\xi,\eta,z,t) \tag{1}$$

$$\left(a_1\frac{\partial}{\partial t}+a_2\right)T(\xi_0,\eta,z,t)=0 \tag{2}$$

$$T(\xi,\eta,\ell/2,t)=T_0\, e^{-\omega t} f(\xi,\eta) \tag{3}$$

$$T(\xi,\eta,-\ell/2,t)=0 \tag{4}$$

in which $T(\xi,\eta,z,t)$ is the temperature of the plate at point (ξ,η,z) at t time, T_0 is the temperature at time $t=0$ on the circumference of the elliptical plate of radius ξ_0 on the upper face, $a_i\,(i=1,2)$ are radiation coeffiecnts, $\omega > 0$ is a constant, λ is the coefficient of thermal conductivity, $\kappa = \lambda/\rho C$ represents thermal diffusivity in which λ is the thermal conductivity of the material, ρ is the density, C is the calorific capacity which is assumed to be constant, and h is the metric coefficient given by:

$$h^2 = 2/[c^2(\cosh 2\xi - \cos 2\eta)] \tag{5}$$

and the ∇^2 denotes the two-dimensional Laplacian operator

$$\nabla^2 = h^2\left(\frac{\partial^2}{\partial \xi^2}+\frac{\partial^2}{\partial \eta^2}\right) \tag{6}$$

2.2 Associated thermal stress problem

The medium is defined by $0 \le \xi \le \xi_0$, $0 \le \eta \le 2\pi$, and $-\ell/2 \le z \le \ell/2$, and compiling various boundary conditions in the elliptical coordinates are defined to determine the influence of thermal boundary conditions on the thermal stresses. Since it is assumed that the cylinder is sufficiently thin, we can introduce the assumption that the plane, initially normal to the middle or neutral plane $(z=0)$ before bending, remains straight and normal to the middle surface during the deformation, and the length of such elements are not altered. This means that the axial stress, which is considered negligible compared with the other stress components, may be neglected in the stress-strain relations. Thus, for solving the quasi-static thermoelasticity problem by using the displacement potential method [11], we assume the potential function $\phi(\xi,\eta,z,t)$ such that it satisfies the equation given below:

$$h^2\nabla^2\phi = \frac{1+\upsilon}{1-\upsilon}\alpha_t T \tag{7}$$

in which G is the shear modulus, υ denotes Poisson's ratio, and α_t is the coefficient of linear expansion, respectively.

The components of the stresses are represented by the use of Goodier's potential stress function $\phi(\xi,\eta,z,t)$ as:

$$\left.\begin{aligned}
(1/h^4)\bar{\sigma}_{\xi\xi} &= -2G(c^2/2)[(\cosh 2\xi - \cos 2\eta)\phi_{,\eta\eta} + \sinh 2\xi\, \phi_{,\xi} - \sin 2\eta\, \phi_{,\eta}],\\
(1/h^4)\bar{\sigma}_{\eta\eta} &= -2G(c^2/2)[(\cosh 2\xi - \cos 2\eta)\phi_{,\xi\xi} - \sinh 2\xi\, \phi_{,\xi} + \sin 2\eta\, \phi_{,\eta}],\\
(1/h^4)\bar{\sigma}_{\xi\eta} &= -2G(c^2/2)[-(\cosh 2\xi - \cos 2\eta)\phi_{,\xi\eta} + \sin 2\xi\, \phi_{,\eta} + \sinh 2\eta\, \phi_{,\xi}]
\end{aligned}\right\} \tag{8}$$

It is observed that the displacements and stresses obtained from equations (7) and (8) do not satisfy the boundary conditions, i.e., the plate should be stress-free. To complement the solution, we found out that the complementary stresses $\bar{\bar{\sigma}}_{ij}$ satisfying the following relations:

$$\bar{\sigma}_{\xi\xi} + \bar{\bar{\sigma}}_{\xi\xi} = 0, \quad \bar{\sigma}_{\xi\eta} + \bar{\bar{\sigma}}_{\xi\eta} = 0 \quad \text{on} \quad \xi = a \tag{9}$$

To solve the isothermal elasticity problem, let us make use of the Airy potential stress function $\chi(\xi,\eta,z,t)$ which satisfies the bi-laplacian equation as:

$$[h^2\nabla^2\chi)]^2 = 0 \tag{10}$$

Then, the complementary stresses in terms of the Airy stress function are given by

$$\begin{aligned}
(1/h^4)\bar{\bar{\sigma}}_{\xi\xi} &= (c^2/2)[(\cosh 2\xi - \cos 2\eta)\,\chi_{,\eta\eta} + \sinh 2\xi\ \chi_{,\xi} - \sin 2\eta\ \chi_{,\eta}],\\
(1/h^4)\bar{\bar{\sigma}}_{\eta\eta} &= (c^2/2)[(\cosh 2\xi - \cos 2\eta)\chi_{,\xi\xi} - \sinh 2\xi\ \chi_{,\xi} + \sin 2\eta\ \chi_{,\eta}],\\
(1/h^4)\bar{\bar{\sigma}}_{\xi\eta} &= (c^2/2)[-(\cosh 2\xi - \cos 2\eta)\chi_{,\xi\eta} + \sin 2\xi\ \chi_{,\eta} + \sinh 2\eta\ \chi_{,\xi}]
\end{aligned} \tag{11}$$

Thus, the final stresses can be represented as

$$\begin{aligned}
\sigma_{\xi\xi} &= \bar{\sigma}_{\xi\xi} + \bar{\bar{\sigma}}_{\xi\xi}\\
\sigma_{\eta\eta} &= \bar{\sigma}_{\eta\eta} + \bar{\bar{\sigma}}_{\eta\eta}\\
\sigma_{\xi\eta} &= \bar{\sigma}_{\xi\eta} + \bar{\bar{\sigma}}_{\xi\eta}
\end{aligned} \tag{12}$$

The equations (1) to (12) constitute the mathematical formulation of the problem under consideration.

3. Solution to the problem

3.1 Solution to the temperature field

We assume that the temperature distribution $T(\xi,\eta,z,t)$ is given by:

$$T = \sum_{n=0}^{\infty}\sum_{m=1}^{\infty} f_n(t)\sin\left[q_{n,m}\left(z+\frac{\ell}{2}\right)+\left(z+\frac{\ell}{2}\right)\right]Ce_{2n}(\xi,q_{n,m})ce_{2n}(\eta,q_{n,m}) \tag{13}$$

in which the function $f_n(t)$ for all time t will be determined later on from the heat conduction equation, $ce_n(\eta,q)$ is the ordinary Mathieu function of the first kind of order n, and $Ce_n(\xi,q)$ is the modified Mathieu function of the second kind of order n. In this case, it is found that the temperature on the face $z=-h/2$ is zero.

By using equation (13) in equation (1), one obtains:

$$f_n(t)_{,t} = -\kappa\alpha_{n,m}^2 f_n(t) \tag{14}$$

in which

$$\alpha_{n,m}^2 = 4q_{n,m}/c^2$$

On integrating equation (14), one obtains

$$f_n(t) = A_{n,m}\exp(-\kappa\alpha_{n,m}^2 t) \tag{15}$$

in which the constant $A_{n,m}$ can be determined from the nature of temperature prescribed on the upper face. Now, by using condition (3), one obtains the function $f(\xi,\eta)$ by the well-known theorem on Fourier's series [1, pp. 296] which can be expressed as:

$$\zeta(\xi,\eta) = T(\xi,\eta,\ell/2,0) = \ell\sum_{n=0}^{\infty}\left[\sum_{m=1}^{\infty} A_{2n,m}Ce_{2n}(\xi,q_{2n,m})ce_n(\eta,q_{2n,m})\right] \tag{16}$$

Both sides of equation (16) are multiplied by $(\cosh 2\xi - \cos 2\eta)\ Ce_p(\xi,q_{p,r})\ ce_p(\eta,q_{p,r})$ and integrated with respect to η from 0 to 2π, and with respect to ξ from 0 to a. Then, by using orthogonal property [1, pp. 175-176], all terms vanish except when $p=n,\ r=m$. Hence,

$$A_{2n,m} = \frac{T_0\exp(-\omega t)\int_0^a\int_0^{2\pi} f(\xi)Ce_{2n}(\xi,q_{2n,m})ce_n(\eta,q_{2n,m})[\cosh 2\xi - \cos 2\eta]\,d\xi\,d\eta}{\pi\ell\int_0^a(\cosh 2\xi - \Theta_{2n,m})Ce_{2n}^2(\xi,q_{2n,m})\,d\xi} \tag{17}$$

and

$$\Theta_{2n,m} = \frac{1}{\pi}\int_0^{2\pi} \cos 2\eta \, ce_{2n}^2(\eta, q_{2n,m})\, d\eta$$
$$= A_0^{(2n)} A_2^{(2n)} + \sum_{r=0}^{\infty} A_{2r}^{(2n)} A_{2r+2}^{(2n)}$$

in which

$ce_{2n}(\eta,q) = \sum_{r=0}^{\infty} A_{2r}^{(2n)} \cos 2r\eta$ is a Mathieu function [1, pp. 27],

$Ce_{2n}(\xi,q) = \sum_{r=0}^{\infty} A_{2r}^{(2n)} \cosh 2r\xi$ is a modified Mathieu function [1, pp. 21],

$q_{2n,m}$ is the root of the transcendental equation $Ce_{2n}(b,q)Fey_{2n}(a,q) - Fey_{2n}(b,q)Ce_{2n}(a,q) = 0$,
and the recurrence relations for the Bessel functions Y_{2r} can be defined as

$$Fey_{2n}(\xi,q) = \sum_{r=0}^{\infty} (A_{2r}^{(2n)} / A_0^{(2n)})\, ce_{2n}(0,q) Y_{2r}(2k\sinh\xi)\ [|\sinh\xi| > 1; R(\xi) > 0]\,.$$

The function given in equation (1) represents the temperature at every instant and all points of a thin elliptical plate of finite height which is subjected to transient temperature on the upper surface $(z = \ell/2)$ with the lower surface $(z = -\ell/2)$ at zero temperature, and the curved surface has homogeneous boundary conditions of the third kind.

3.2 Solution to the thermal stresses

By referring to the fundamental equation (1) and its solution (13) for the heat conduction equation, the solution for the displacement function is represented by Goodier's displacement potential $\phi(\xi,\eta,z,t)$, referred to by equation (8) as

$$\phi = -\alpha t\left(\frac{1+\nu}{1-\nu}\right)c^2h^2 \sum_{n=0}^{\infty}\sum_{m=1}^{\infty} \overline{f}(q_{n,m}) \sin\left[q_{n,m}\left(z+\frac{h}{2}\right)+\left(z+\frac{h}{2}\right)\right]$$
$$\times C_{e_{2n}}(\xi,q_{n,m})\, c_{e_{2n}}(\eta,q_{n,m}) \exp[(-k\alpha_{2n,m}^2+\omega)t]/4q_{2n,m}C_{n,m} \tag{18}$$

Now, assume Airy's stress function $\chi(\xi,\eta,z,t)$ which satisfies condition (10) as

$$\chi = \sum_{n=0}^{\infty}\sum_{m=1}^{\infty} \overline{f}(q_{n,m}) C_{e_{2n}}(\xi,q_{n,m})\, c_{e_{2n}}(\eta,q_{n,m}) \Bigg\{ X_{n,m}$$
$$\times\sinh\left[q_{n,m}\left(z+\frac{h}{2}\right)+\left(z+\frac{h}{2}\right)\right] + zY_{n,m}\cosh\left[q_{n,m}\left(z+\frac{h}{2}\right)+\left(z+\frac{h}{2}\right)\right]\Bigg\} \tag{19}$$
$$\times\exp[(-k\alpha^2{}_{2n,m}+\omega)t]/C_{n,m}$$

in which $X_{n,m}$ and $Y_{n,m}$ are the arbitrary functions that can finally be determined by using condition (9).

$$X_{n,m} = -\frac{G\alpha_t c^2 h^2}{2q_{2n,m}}\left(\frac{1+\nu}{1-\nu}\right),\ Y_{n,m} = 0 \tag{20}$$

By substituting $X_{n,m}$ and $Y_{n,m}$ from equation (20) into equation (19) we get the final Airy's function as

$$\chi = -G\alpha_t \sum_{n=0}^{\infty}\sum_{m=1}^{\infty} c^2h^2\left(\frac{1+\nu}{1-\nu}\right)\overline{f}(q_{n,m}) C_{e_{2n}}(\xi,q_{n,m})\, c_{e_{2n}}(\eta,q_{n,m})$$
$$\times\sinh\left[q_{n,m}\left(z+\frac{h}{2}\right)+\left(z+\frac{h}{2}\right)\right]\exp[(-k\alpha_{2n,m}^2+\omega)t]/2q_{2n,m}C_{n,m} \tag{21}$$

Using equations (8) and (18), one obtains the stresses due to temperature as:

$$\begin{aligned}\bar{\sigma}_{\xi\xi} &= -c^2 G h^4 \cosh 2\xi + \frac{c^4 h^6}{4q_{2n,m} C_{n,m}} G\alpha_t \left(\frac{1+\nu}{1-\nu}\right) \sum_{n=0}^{\infty} \sum_{m=1}^{\infty} \bar{f}(q_{2n,m}) \\ &\times \sin[\tfrac{1}{2}(h+2z)(1+\gamma)]\{(\cos 2\eta) ce''_{2n}(\eta, q_{2n,m}) Ce_{2n}(\xi, q_{2n,m}) \\ &+ ce_{2n}(\eta, q_{2n,m}) Ce'_{2n}(\xi, q_{2n,m}) \sin 2\xi - Ce_{2n}(\xi, q_{2n,m}) \\ &\times ce'_{2n}(\eta, q_{2n,m}) \sin 2\eta\} \exp[-(k\alpha^2_{2n,m} + \omega)t]\end{aligned} \tag{22}$$

$$\begin{aligned}\bar{\sigma}_{\eta\eta} &= -c^2 G h^4 \cosh 2\xi - \frac{c^4 h^6}{4q_{2n,m} C_{n,m}} G\alpha_t \left(\frac{1+\nu}{1-\nu}\right) \sum_{n=0}^{\infty} \sum_{m=1}^{\infty} \bar{f}(q_{2n,m}) \\ &\times \sin[\tfrac{1}{2}(h+2z)(1+\gamma)]\{(\cos 2\eta) ce_{2n}(\eta, q_{2n,m}) Ce'_{2n}(\xi, q_{2n,m}) \\ &+ ce_{2n}(\eta, q_{2n,m}) Ce'_{2n}(\xi, q_{2n,m}) \sin 2\xi - Ce_{2n}(\xi, q_{2n,m}) \\ &\times ce'_{2n}(\eta, q_{2n,m}) \sin 2\eta\} \exp[-(k\alpha^2_{2n,m} + \omega)t]\end{aligned} \tag{23}$$

$$\begin{aligned}\bar{\sigma}_{\xi\eta} &= \frac{c^4 h^6}{4q_{2n,m} C_{n,m}} G\alpha_t \left(\frac{1+\nu}{1-\nu}\right) \sum_{n=0}^{\infty} \sum_{m=1}^{\infty} \bar{f}(q_{2n,m}) \\ &\times \sin[\tfrac{1}{2}(h+2z)(1+\gamma)]\{(\cos 2\eta - \cosh 2\xi) ce'_{2n}(\eta, q_{2n,m}) \\ &\times Ce'_{2n}(\xi, q_{2n,m}) + ce_{2n}(\eta, q_{2n,m}) Ce'_{2n}(\xi, q_{2n,m}) \\ &\times \sin 2\eta + Ce_{2n}(\xi, q_{2n,m}) ce'_{2n}(\eta, q_{2n,m}) \sin 2\xi\} \\ &\times \exp[-(k\alpha^2_{2n,m} + \omega)t]\end{aligned} \tag{24}$$

Using equations (11) and (21), one obtains the thermal complementary stresses as:

$$\begin{aligned}\bar{\bar{\sigma}}_{\xi\xi} &= -\frac{G\alpha_t c^4 h^6}{4q_{2n,m} C_{n,m}} \left(\frac{1+\nu}{1-\nu}\right) \sum_{n=0}^{\infty} \sum_{m=1}^{\infty} \bar{f}(q_{2n,m}) \sin[\tfrac{1}{2}(h+2z)(1+\gamma)] \\ &\times \{(\cos 2\eta - \cosh 2\xi) ce''_{2n}(\eta, q_{2n,m}) Ce_{2n}(\xi, q_{2n,m}) \\ &+ ce_{2n}(\eta, q_{2n,m}) Ce'_{2n}(\xi, q_{2n,m}) \sin 2\xi - Ce_{2n}(\xi, q_{2n,m}) \\ &\times ce'_{2n}(\eta, q_{2n,m}) \sin 2\eta\} \exp[-(k\alpha^2_{2n,m} + \omega)t]\end{aligned} \tag{26}$$

$$\begin{aligned}\bar{\bar{\sigma}}_{\eta\eta} &= -\frac{G\alpha_t c^4 h^6}{4q_{2n,m} C_{n,m}} \left(\frac{1+\nu}{1-\nu}\right) \sum_{n=0}^{\infty} \sum_{m=1}^{\infty} \bar{f}(q_{2n,m}) \sin[\tfrac{1}{2}(h+2z)(1+\gamma)] \\ &\times \{-(\cos 2\eta - \cosh 2\xi) ce_{2n}(\eta, q_{2n,m}) Ce''_{2n}(\xi, q_{2n,m}) \\ &- ce_{2n}(\eta, q_{2n,m}) Ce'_{2n}(\xi, q_{2n,m}) \sin 2\xi \\ &+ Ce_{2n}(\xi, q_{2n,m}) ce'_{2n}(\eta, q_{2n,m}) \sin 2\eta\} \\ &\times \exp\{-[k\alpha^2_{2n,m} + \omega]t\}\end{aligned} \tag{27}$$

$$\begin{aligned}\bar{\bar{\sigma}}_{\xi\eta} &= -\frac{G\alpha_t c^4 h^6}{4q_{2n,m} C_{n,m}} \left(\frac{1+\nu}{1-\nu}\right) \sum_{n=0}^{\infty} \sum_{m=1}^{\infty} \bar{f}(q_{2n,m}) \sin[\tfrac{1}{2}(h+2z)(1+\gamma)] \\ &\times \{(\cos 2\eta - \cosh 2\xi) ce'_{2n}(\eta, q_{2n,m}) Ce'_{2n}(\xi, q_{2n,m}) \\ &+ ce_{2n}(\eta, q_{2n,m}) Ce'_{2n}(\xi, q_{2n,m}) \sin 2\eta \\ &+ Ce_{2n}(\xi, q_{2n,m}) ce'_{2n}(\eta, q_{2n,m}) \sin 2\xi\} \\ &\times \exp\{-[k\alpha^2_{2n,m} + \omega]t\}\end{aligned} \tag{28}$$

By substituting equations (22-27) into equation (12) we obtain the complete solution in terms of the displacement potential ϕ and the stress function χ as:

$$\begin{aligned}\sigma_{\xi\xi} &= \frac{G\alpha_t c^4 h^6}{4q_{2n,m} C_{n,m}}\left(\frac{1+\nu}{1-\nu}\right)\sum_{n=0}^{\infty}\sum_{m=1}^{\infty}\bar{f}(q_{2n,m})(\sin[\tfrac{1}{2}(h+2z)(1+\gamma)] \\ &\quad -\sinh[\tfrac{1}{2}(h+2z)(1+\gamma)])\{-(\cos 2\eta-\cosh 2\xi)ce''_{2n}(\eta,q_{2n,m}) \\ &\quad \times Ce_{2n}(\xi,q_{2n,m})+ce_{2n}(\eta,q_{2n,m})Ce'_{2n}(\xi,q_{2n,m})\sin 2\xi \\ &\quad -Ce_{2n}(\xi,q_{2n,m})ce'_{2n}(\eta,q_{2n,m})\sin 2\eta\}\exp[-(k\alpha^2_{2n,m}+\omega)t]\end{aligned} \tag{29}$$

$$\begin{aligned}\sigma_{\eta\eta} &= -\frac{G\alpha_t c^4 h^6}{4q_{2n,m} C_{n,m}}\left(\frac{1+\nu}{1-\nu}\right)\sum_{n=0}^{\infty}\sum_{m=1}^{\infty}\bar{f}(q_{2n,m})(\sin[\tfrac{1}{2}(h+2z)(1+\gamma)] \\ &\quad -\sinh[\tfrac{1}{2}(h+2z)(1+\gamma)])\{(\cos 2\eta-\cosh 2\xi)ce_{2n}(\eta,q_{2n,m}) \\ &\quad \times Ce''_{2n}(\xi,q_{2n,m})+ce_{2n}(\eta,q_{2n,m})Ce'_{2n}(\xi,q_{2n,m})\sin 2\xi \\ &\quad -Ce_{2n}(\xi,q_{2n,m})ce'_{2n}(\eta,q_{2n,m})\sin 2\eta\}\exp[-(k\alpha^2_{2n,m}+\omega)t]\end{aligned} \tag{30}$$

$$\begin{aligned}\sigma_{\xi\eta} &= \frac{G\alpha_t c^4 h^6}{4q_{2n,m} C_{n,m}}\left(\frac{1+\nu}{1-\nu}\right)\sum_{n=0}^{\infty}\sum_{m=1}^{\infty}\bar{f}(q_{2n,m})(\sin[\tfrac{1}{2}(h+2z)(1+\gamma)] \\ &\quad -\sinh[\tfrac{1}{2}(h+2z)(1+\gamma)])\{(\cos 2\eta-\cosh 2\xi)ce'_{2n}(\eta,q_{2n,m}) \\ &\quad \times Ce'_{2n}(\xi,q_{2n,m})+ce_{2n}(\eta,q_{2n,m})Ce'_{2n}(\xi,q_{2n,m})\sin 2\eta \\ &\quad +Ce_{2n}(\xi,q_{2n,m})ce'_{2n}(\eta,q_{2n,m})\sin 2\xi\}\exp[-(k\alpha^2_{2n,m}+\omega)t]\end{aligned} \tag{31}$$

4. Transition to circular plate

When the elliptical plate tends to a circular plate of the radius ξ_0, the semi-focal $c \to 0$ and then α_m is the root of the transcendental equation $J_0(\alpha_m)=0$. Also $e \to 0$ [as $\xi \to \infty$], $\cosh 2\xi\, d\xi \to$ $2\cosh 2\xi \sinh 2\xi\, d\xi \to 2r dr / c^2$, $\sinh\xi \to \cosh\xi$, $h\cosh\xi \to r$ [as $h \to 0$], $\cosh\xi\, d\xi \to r\, dr$, $h\sinh\xi\, d\xi \to dr$,

By using results from [12] we obtain:

$$Ce_0(\xi,q_{0,m}) \to p'_0 J_0(\lambda_m r),\ Ce'_0(\xi,q_{0,m}) \to p'_0 J'_0(\lambda_m r),\ Ce''_0(\xi,q_{0,m}) \to p'_0 J''_0(\lambda_m r),\ ce_0(\eta,q_m) \to 1/\sqrt{2},$$

$$A_0^{(0)} \to 1/\sqrt{2}, A_2^{(0)} \to 0,\ \Theta_{2m} \to 0,\ \lambda^2_{0,m} = \alpha^2_{0,m}/a^2 = \alpha^2_m/a^2 = \lambda^2_m,\ p'_0 = Ce_0(0,q_{0,m})ce_0(2\pi,q_{0,m})/A_0^{(0)}.$$

Taking into account the parameters above, the temperature distribution in the cylindrical coordinate is finally represented by:

$$T(r,z,t) = \sum_{n=0}^{\infty}\sum_{m=1}^{\infty} f_n(t)\sin\left[\lambda_m\left(z+\frac{\ell}{2}\right)+\left(z+\frac{\ell}{2}\right)\right]p'_0 J_0(\lambda_m r) \tag{32}$$

in which

$$f_n(t) = A_{n,m}\exp(-\kappa\lambda_m^2 t),$$

$$A_m = \frac{T_0\exp(-\omega t)\int_0^a r\, p'_0 J_0(\lambda_m r) f(r)\, dr}{\pi\ell\int_0^a r[p'_0 J_0(\lambda_m r)]^2\, dr}$$

The aforementioned degenerated result agrees with the previous result [13].

5. Numerical Results, Discussion, and Remarks

For the purpose of simplicity of calculation, the following dimensionless values are introduced:

$$\left.\begin{array}{l}\bar{\xi}=\xi/\xi_0,\ \bar{z}=z/\xi_0,\ e=c/\xi_0,\ \tau=\kappa t/\xi_0{}^2,\\ \bar{\theta}=T/T_0, \bar{\sigma}_{ij}=\sigma_{ij}/E\alpha\theta_0\ \ (i,j=\xi,\eta)\end{array}\right\} \tag{33}$$

By substituting the value of equation (33) into equation (13) and components of stresses, we obtained the expressions for temperature and the thermal stresses, respectively, for our numerical discussion. The numerical computations have been carried out for an Aluminum (pure) elliptical plate with the physical parameter as $\xi_0 = 1$ m, $\ell = 0.08$ m, reference temperature as 150 0C, and $f(\xi,\eta)=\delta(\xi-\xi_i)\delta(\eta-\eta_i)$ in which $0\le\xi_i\le\xi_0$ and $0\le\eta_i\le 2\pi$. The thermo-mechanical properties are considered as modulus of elasticity E = 70 GPa, Poisson's ratio υ = 0.35, thermal expansion coefficient α = 23×10-6 /0C, thermal diffusivity κ = 84.18 m2s−1, and thermal conductivity λ = 204.2 Wm−1K−1. The $q_{2n,m} = 0.0986$, 0.3947, 0.8882, 1.5791, 2.4674, 3.5530, 4.8361, 6.3165, 7.9943, 9.8696, 11.9422, 14.2122, 16.6796, 19.3444, 22.2066, 25.2661, 28.5231, 31.9775, 35.6292, and 39.4784 are the positive and real roots of the transcendental equation $Ce_{2n}(a,q)=0$. In order to examine the influence of heating on the plate, the numerical calculations were performed for all the variables, and the numerical calculations are depicted in the following figures with the help of MATHEMATICA software. Figures 2–5 illustrate the numerical results of the temperature distribution and stresses of the elliptical plate under the thermal boundary condition that are subjected to arbitrary initial temperature on the upper face while keeping lower face at zero temperature. Figure 2(a) indicates the temperature distribution along the direction of $\bar{z}$-axis of the plate. The maximum values of temperature magnitude arise from the upper face due to additional heat supply. The distribution of temperature gradient at each instance decreases the axial direction tending and attains its minimum at the lower face which is kept at zero temperature.

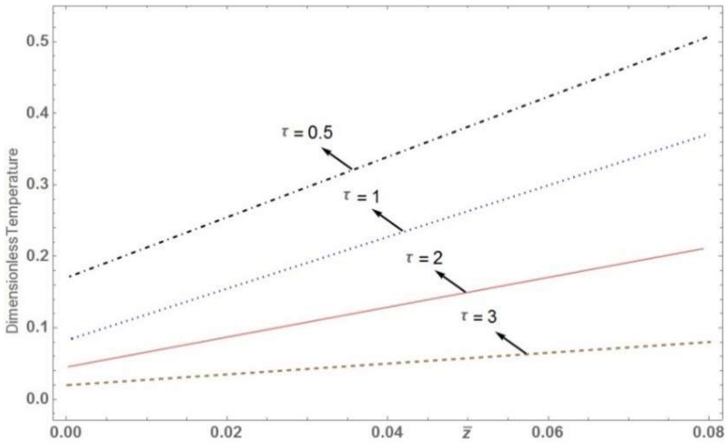

Fig. 2(a). Temperature distribution $\bar{\theta}$ along $\bar{z}$ for different values of τ

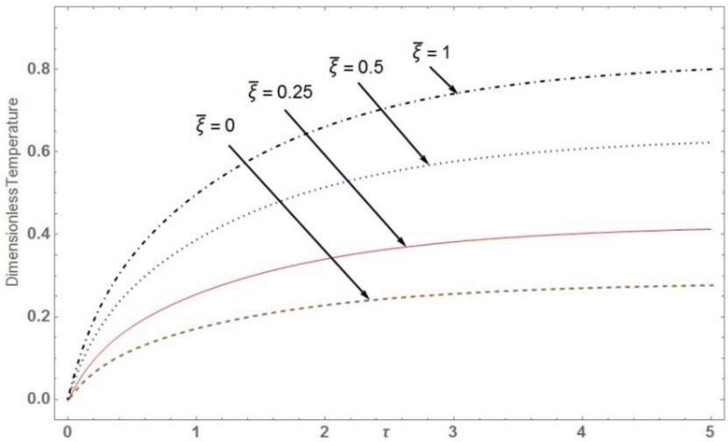

Fig. 2(b). Temperature distribution $\bar{\theta}$ along τ for different values of $\bar{\xi}$

Fig. 2(b) illustrates the temperature profile along the time direction for various values of the radius. Temperature trend increases along the time direction from inner core to the outer curved surface irrespective of the angular direction for a fixed value of $\bar{z}$. At the outer part of the thickness, temperature fluctuation seems more stable due to the accumulation of energy which is caused by more exposure to heat sources; hence, thermal expansion is more at the outer part of the plate which gives high tensile force. Figure 3(a) depicts that the radial stress $\bar{\sigma}_{\xi\xi}$ attains its minimum at the outer core due to the compressive forces occurring at the outer region. Figure 3(b) indicates the dimensionless radial stress along the angular direction for different values of the thickness; it is clear that the radial stress follows the sinusoidal nature due to the periodicity of Mathieu function.

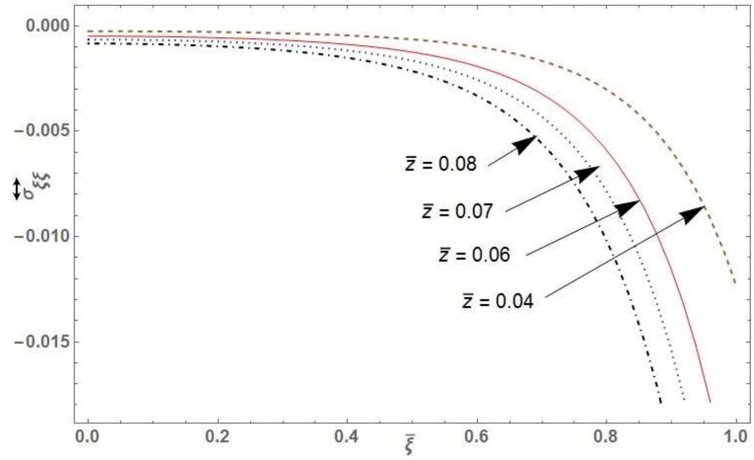

Fig. 3(a). Dimensionless radial stress along $\bar{\xi}$ for different values of $\bar{z}$

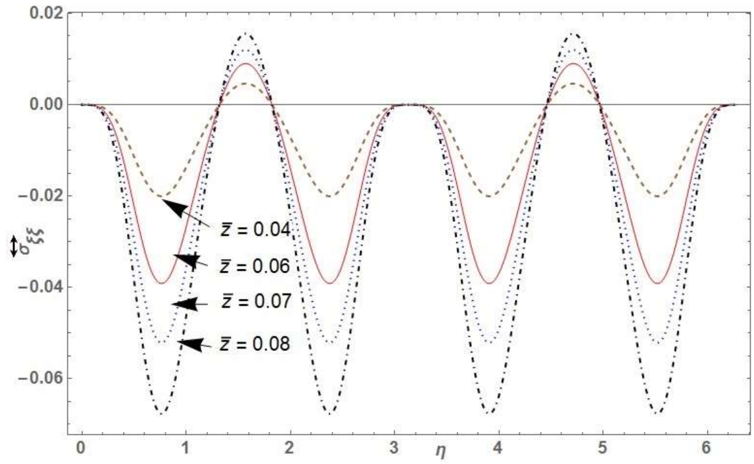

Fig. 3(b). Dimensionless radial stress along η for various values of $\bar{z}$

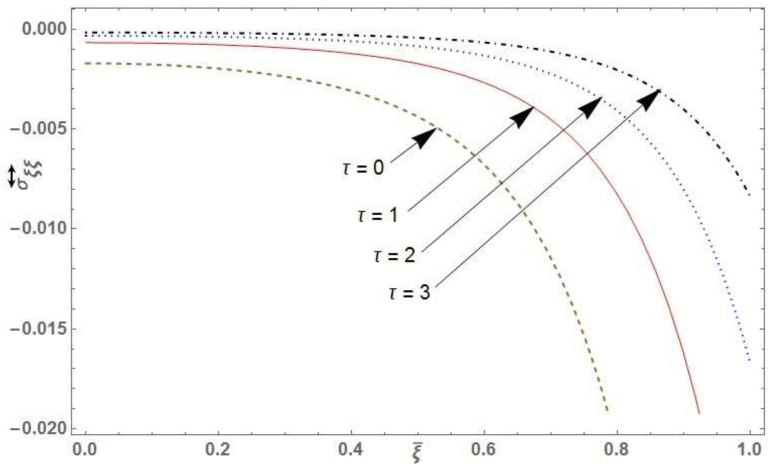

Fig. 3(c). Dimensionless radial stress along $\bar{\xi}$ for different values of τ

Figure 3(c) shows the dimensionless radial stress along the radial direction for different time series; the stress attains its maximum at the core of the inner part which may be due to initial temperature, and lowers towards the outer part for different time series along the radial direction. Figure 3(d) depicts the dimensionless radial stress along the time series for different radii;

the stress increases gradually with the increase in time for different radii and stabilizes after a certain time due to the rate of temperature change with respect to time.

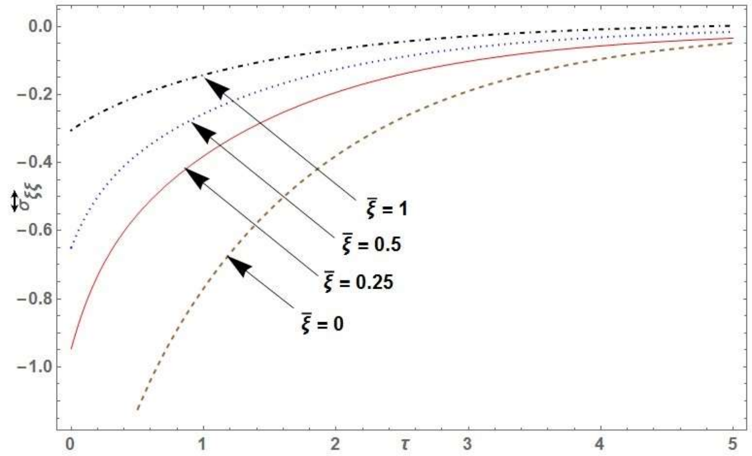

Fig. 3(d). Dimensionless radial stress along τ for different values of $\bar{\xi}$

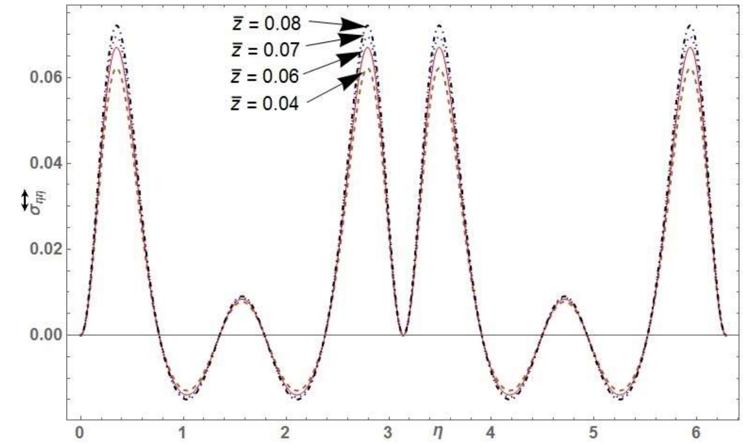

Fig. 4(a). Dimensionless tangential stress along η for different values of $\bar{z}$

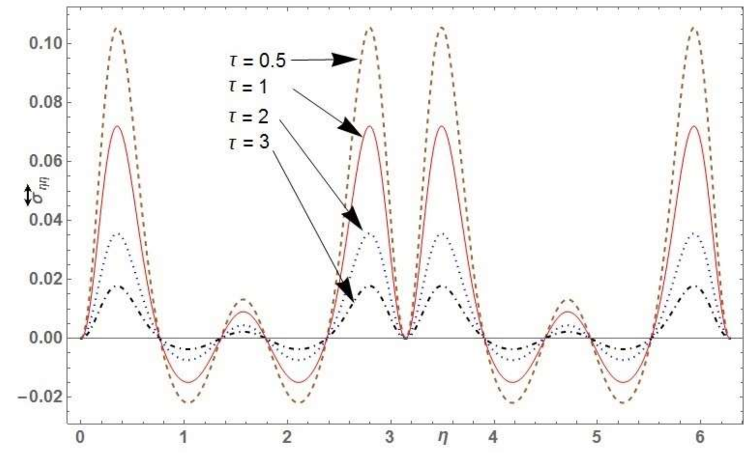

Fig. 4(b). Dimensionless tangential stress along η for different values of τ

Figures 4(a) and 4(b) represent dimensionless tangential stress; both graphs are sinusoidal in nature showing vibration of the plate due to the periodicity of Mathieu function. Figure 4(c) gives the dimensionless tangential stress along time series for different radii; it is shown that tangential stresses are maximum at inner core of the plate and lower towards the outer end and stabilize after a certain time.

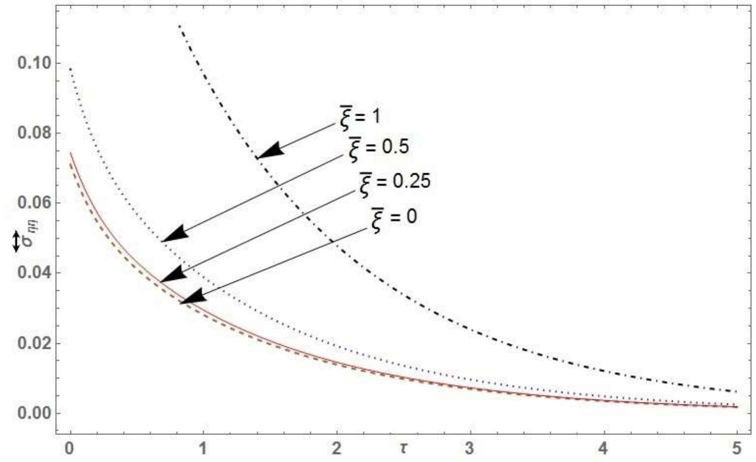

Fig. 4(c). Dimensionless tangential stress along τ for different values of $\bar{\xi}$

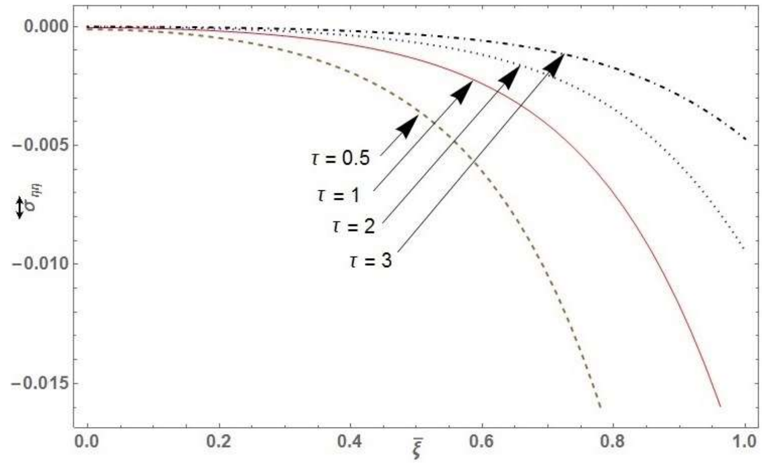

Fig. 4(d). Dimensionless tangential stress along $\bar{\xi}$ for different values of τ

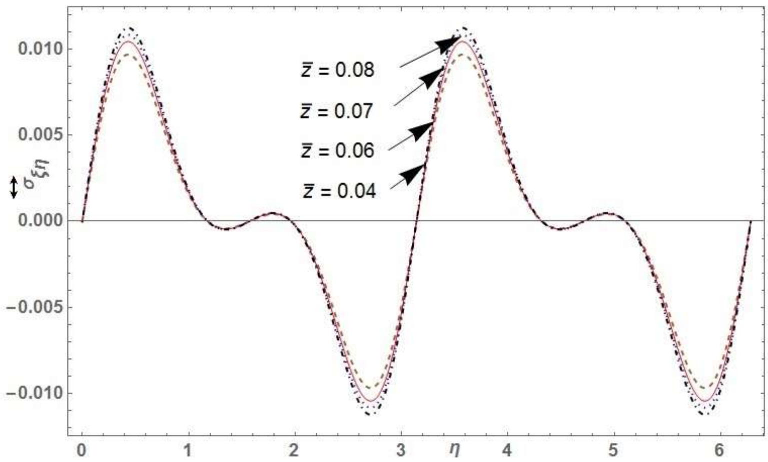

Fig. 5(a). Shear stress $\bar{\sigma}_{\xi\eta}$ along η for different values of $\bar{z}$

Figure 5(a) represents dimensionless shear stress profile. The graph is sinusoidal in nature showing vibration of the plate due to the periodicity of Mathieu function. Figures 5(b) and 5(c) indicate the shear stress along $\bar{\xi}$ - direction of the plate for different values of $\bar{z}$ and time. The maximum value of stress magnitude occurs at the outer edge due to the additional heat energy throughout the body. The distribution of stress at every point of $\bar{z}$ and time decreases towards the central part of the ellipse boundary; thus, it tends to zero at the unheated part. Figure 5(d) depicts that the shear stress $\bar{\sigma}_{\xi\eta}$ attains zero at $\eta = 0,\ \pi/2,\ \pi,\ 3\pi/2, 2\pi$, whereas on the other parts, it attains its maximum due to the accumulation of thermal energy dissipated by sectional.

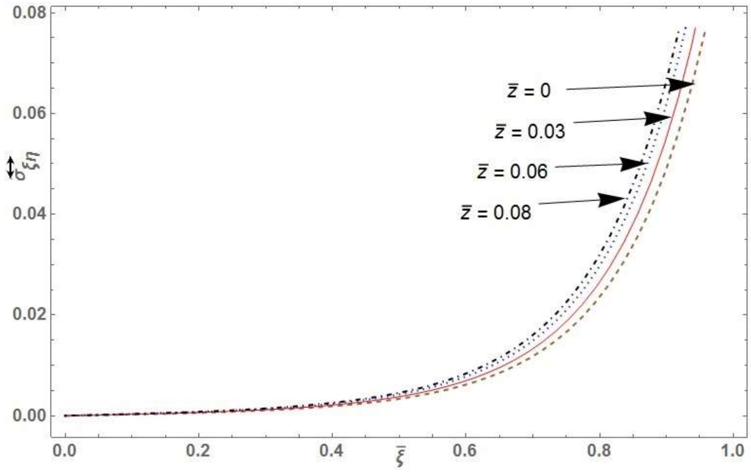

Fig. 5(b). Shear stress $\ddot{\sigma}_{\xi\eta}$ along $\bar{\xi}$ for various values of $\bar{z}$

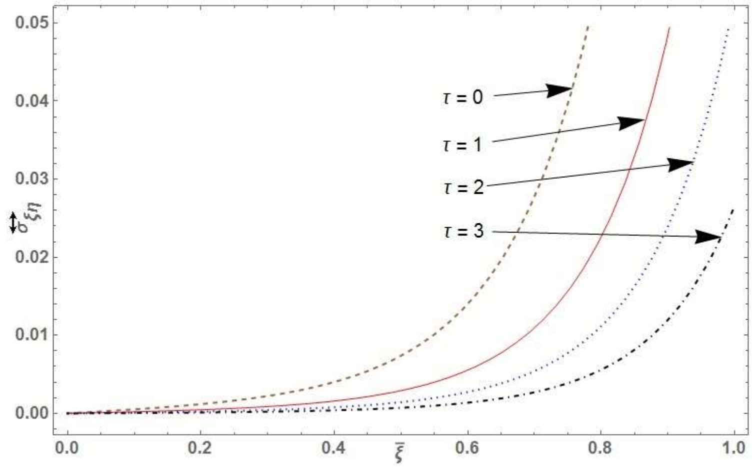

Fig. 5(c). Shear stress $\ddot{\sigma}_{\xi\eta}$ along $\bar{\xi}$ for different values of τ

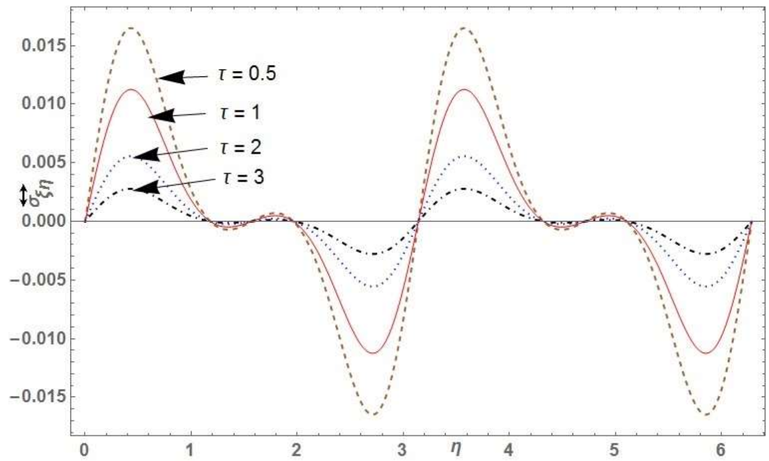

Fig. 5(d). Shear stress $\ddot{\sigma}_{\xi\eta}$ along η for various values of τ

6. Conclusion

In this manuscript, we have described the theoretical treatment of the quasi-static thermal stresses in a thin elliptical plate. The temperature distribution and the stresses in the form of ordinary and the modified Mathieu functions are used to determine the solution by classical methods. The analytical technique proposed here is relatively straightforward and widely applicable compared with the methods proposed by other researchers. The results obtained while carrying out the research are generalized as follows:

• The advantage of this approach is its generality and its mathematical power to handle different types of mechanical and thermal boundary conditions during induced stresses under thermal loading.

- The maximum tensile stress shifts from the outer surface due to maximum expansion of the outer part of the plate, and its absolute value increases with the radius. This shifting of stress could be due to heat, stresses, concentration, or available internal heat sources under the known temperature field.
- Finally, the maximum tensile stress occurs in the circular core on the major axis compared with the elliptical core indicating the weak distribution of heat. This difference might be due to insufficient penetration of heat through the elliptical inner surface.
- The aforementioned thermal stress calculation concept can be beneficial in the field of micro-devices or microsystem applications, planar continuum robots, prediction of the elastoplastic bending, and so forth.

Acknowledgement

Scholar student Mrs. Tara Dhakate (Maths dept., MG College-Armori) double checked every single equation in the paper using Mathematica. Her help is greatly appreciated.

References

[1] Gupta, R.K., A finite transform involving Mathieu functions and its application, *Proc. Net. Inst. Sc., India, Part A*, 30(6), 1964, pp. 779-795.

[2] El Dhaba, A.R., Ghaleb, A.F., Abou-Dina, M.S., A problem of plane, uncoupled linear thermoelasticity for an infinite, elliptical cylinder by a boundary integral method, *Journal of Thermal Stresses*, 26(2), 2003, pp. 93-121.

[3] Sato, K., Heat conduction in an infinite elliptical cylinder during heating or cooling, *Proceedings of the 55th Japan National Congress on Theoretical and Applied Mechanics*, 55, 2006, pp. 157-158.

[4] Helsing, J., Integral equation methods for elliptic problems with boundary conditions of mixed type, *Journal of Computational Physics*, 228(23), 2009, pp. 8892-8907.

[5] Dang, Q.A., Mai, X.T., Iterative method for solving a problem with mixed boundary conditions for biharmonic equation arising in fracture mechanics, *Boletim da Sociedade Paranaense de Matemática*, 31(1), 2013, pp. 65–78.

[6] Al Duhaim, H.R., Zaman, F.D., Nuruddeen, R.I., Thermal stress in a half-space with mixed boundary conditions due to time dependent heat source, *IOSR Journal of Mathematics*, 11(6), 2015, pp. 19-25.

[7] Parnell, W.J., Nguyen, V.-H., Assier, R., Naili, S., Abrahams, I.D., Transient thermal mixed boundary value problems in the half-space, *SIAM Journal on Applied Mathematics*, 76(3), 2016, pp. 845–866.

[8] Nuruddeen, R.I., Zaman, F.D., Temperature distribution in a circular cylinder with general mixed boundary conditions, *Journal of Multidisciplinary Engineering Science and Technology*, 3(1), 2016, pp. 3653-3658.

[9] Bhad, P.P., Varghese, V., Khalsa, L.H., Heat source problem of thermoelasticity in an elliptic plate with thermal bending moments, *Journal of Thermal Stresses*, 40(1), 2016, pp. 96-107.

[10] Bhad, P.P., Varghese, V., Khalsa, L.H., Thermoelastic-induced vibrations on an elliptical disk with internal heat sources, *Journal of Thermal Stresses*, 40(4), 2016, pp. 502-516.

[11] Ventsel, E., Krauthammer, T., *Thin Plates and Shells: Theory, Analysis, and Applications*, Marcel Dekker, New York, 2001.

[12] McLachlan, N.W., *Theory and Application of Mathieu function*, Clarendon Press, Oxford, 1947.

[13] Bhad, P.P., Varghese, V., Thermoelastic analysis on a circular plate subjected to annular heat supply, *Global Journal for Research Analysis*, 3(4), 2014, pp. 141-145.